Tuning the extent and depth of penetration of flexible liposomes in human skin

Silvia Franzé[1], Giulia Donadoni[1], Alessandro Podestà[2], Patrizia Procacci[3], Marica Orioli[1], Marina Carini[1], Paola Minghetti[1], Francesco Cilurzo[1]*

[1]Department of Pharmaceutical Sciences, Università degli Studi di Milano, via G. Colombo 71, 20133 Milano, Italy

[2]Department of Physics and CIMaINa, Università degli Studi di Milano, via Celoria 16, 20133 Milano, Italy

[3]Biomedical Sciences for Health, Università degli Studi di Milano, via G. Colombo 71, 20133 Milano, Italy

*Correspondence to: Francesco Cilurzo (Address: Via G. Colombo, 71 – 20133 Milan, Italy; Telephone: +390250324635; Fax: +390250324657; E-mail: francesco.cilurzo@unimi.it)

Abstract

In this work we made an attempt to assess the effect of drug-induced changes of flexibility on the penetration of deformable vesicles into the human skin. Eight cationic liposomes with different degrees of flexibility were obtained by entrapping unfractionated heparin, enoxaparin and nadroparin. The deformability was studied by a novel, facile and reliable extrusion assay appositely developed and validated by means of quantitative nanoscale mechanical AFM measurements of vesicle elastic modulus ($\log_{10}$(YM)). The proposed extrusion assay, determining the forces involved in vesicles deformation, resulted very sensitive to evidence minimal changes in bilayer rigidity (σ) and vesicle deformation (K).

The drug loading caused a reduction of liposome flexibility with respect to the reference plain liposomes and in accordance to the heparin type, drug to cationic lipid (DOTAP) ratio and drug distribution within the vesicles. Interestingly, the σ and $\log_{10}$(YM) values perfectly correlated (R^2=0.935), demonstrating the reliability of the deformability data obtained with both approaches. The combination of TEM and LC-MS/MS spectrometry allowed the pattern of the penetration of the entire vesicles into the skin to be followed. In all cases, intact liposomes in the epidermis layers were observed and a relationship between the depth of penetration and the liposome flexibility was found, supporting the hypothesis of the whole vesicles penetration mechanism. Moreover, the results of the extent (R_{24}) of vesicle penetration in the human skin samples showed a direct relation to the flexibility values (σ_1= 0.65 ± 0.10 MPa→R_{24}=3.33 ± 0.02 µg/mg; σ_2=0.95 ± 0.04 MPa→R_{24}=1.18 ± 0.26 µg/mg; σ_3=1.89 ± 0.30 MPa→R_{24}=0.53 ± 0.33 µg/mg).

Keywords: flexible liposomes; human skin penetration; deformation; Peak Force Tapping (PFT) AFM; Young's modulus; heparin

Introduction

The human skin is an excellent barrier evolved to exert a protective function against the external environment, limiting the absorption of exogenous molecules. Nanotechnologies have been proposed to escape the defences of the skin, taking advantage of some defects of the stratum corneum which, at microscopic level, might be seen as a poorly permeable nano-porous membrane[1]. In fact in some regions, the corneocytes are not perfectly overlapped and some channel-like pores with a higher water content are formed. This adds to the hydrophilic tiny furrows (0.4-36 nm large) present in the intercellular spaces between the polar heads of the stratum corneum lipids[1]. Among nanocarriers, liposomes, owing to their particular composition, have been considered as the most suitable means to enhance the skin penetration of drugs because of a number of intrinsic potentialities. First, the fusion of the vesicles with the lipid components of the stratum corneum increases the moisture content, similarly to the application of fat occlusive formulations, thus widening the intercellular pores between corneocytes. Secondly, liposomes increase the solubility of drugs on the skin surface, favouring their partition into the skin[2]. Finally, they may form a local depot of drug, allowing a sustained release and the reduction of the number of dose administrations[3]. However, it is now recognized that conventional liposomes, having a rigid bilayer, mostly disassemble on the skin surface and fail to enhance skin drug absorption[4]. Thus, novel generations of lipid vesicles have been proposed to solve this issue[4-5]. Among them, flexible liposomes are of increasing interest. These vesicles are composed mainly of amphiphilic molecules forming bilayers with the addition of non-ionic, single chain surfactants with high curvature radius, claimed to have deformable properties. With respect to conventional liposomes, flexible liposomes can adapt their structure to support relatively high stress because the surfactant relocates in the zones of maximum pressure allowing shape changes at minimum energetic cost[6]. Then, it is supposed that flexible liposomes can reversibly deform in at least one direction, whilst remaining as intact vesicles to pass through the narrow pores of the stratum corneum[7]. However, this mechanism of penetration is still questioned[6] and a real evidence of the possible relationship existing between the level of flexibility of the liposomes and their qualitative and quantitative penetration into human skin is missing.

In this work the role exerted by the degree of vesicle deformation on the extent and depth of penetration of flexible liposomes was investigated. In particular, attention was focused on the development of novel approaches to assess the liposome deformability and the penetration of intact vesicles into human skin. The study was performed by designing a series of cationic liposomes with different degrees of deformability, tuned by entrapping three heparins with different physicochemical features[8].

Cationic flexible liposomes were used because they seem to assure a greater skin penetration of several compounds with respect to neutral and/or anionic liposomes[9-11].

Heparins were chosen since glycosaminoglycans exhibit a high affinity for cationic lipids and therefore can severely influence the physicochemical features of liposomes in terms of ζ-potential, aggregation state and

stability[12-13]. It is then expected that the complexation between drug and lipid components would affect the ability of the lipid bilayer to rearrange its structure, thus altering its elastic properties. Moreover, heparins were selected as model compounds since they are not able to cross the skin due to their unfavourable physicochemical properties[8]. Finally, within this class of drugs, it is possible to select some molecules having similar structure but very different characteristics such as molecular weight, surface charge and chemical residues[14], which overall may differently impact on the bilayer fluidity of flexible liposomes. Finally, Tween® 80 was used as edge activator since it provides softer structures with respect to other surfactants commonly used in these formulations, such as sodium cholate or Span[15-16].

To systematically study the flexibility of the vesicles, a combined approach based on the Atomic Force Microscopy (AFM) and a novel dynamometer assisted extrusion assay was exploited.

The pattern of penetration of the intact vesicles was determined by combining the results obtained by an appositely developed HPLC-ESI-MS/MS method for the quantification of exogenous lipids in the biological sample, with those of TEM imaging technique.

Material and Methods

Materials. 1,2-dioleoyl-3-trimethylammonium-propane (DOTAP) (Avanti Polar Lipids, Inc.); 1,2-dipalmitoyl-sn-glycero-3-phosphoethanolamine-N-(glutaryl) (Glutaryl PE) (Avanti Polar Lipids, Inc); Tween® 80 (Croda chocques, France); egg- Phosphatidylcholine (egg-PC) and sodium tetraborate decahydrate (Sigma-Aldrich®, Italy); Sodium enoxaparin (Clexane® 10000 IU/mL, Sanofi Aventis, Italy), calcium nadroparin (Fraxiparina 19500 IU/mL, Glaxo-SmithKline, Italy), sodium unfractionated heparin (UFH) (kindly provided by LDO S.p.A., Milan, Italy). HPLC-grade and analytical-grade organic solvents were also purchased from Sigma-Aldrich (Milan, Italy). HPLC-grade water was prepared with a Milli-Q water purification system. Carbazole was purchased from Merck, Italy. Osmium tetroxide (OsO_4) (Sigma-Aldrich, Italy). All other reagents were of analytical grade unless specified.

Preparation of liposomes

Flexible cationic liposomes were prepared according to the conventional thin film hydration method. Lipids (DOTAP: glutaryl PE 99:1 mol/mol) and Tween® 80 were dissolved in chloroform and the organic solvent was evaporated under reduced pressure (80 mBar) for 1 hour using a rotavapor (RII, Buchi, Italy). The lipid film was rehydrated with an aqueous solution of drug or pure water (in the case of plain liposomes) to yield a 1% w/v lipid concentration in the final suspension (Table 1). Lipids were left to swell overnight at 4°C prior to manually extruding the liposomes (Avanti® Mini-Extruder, Avanti Polar Lipids, Inc.) by passing the samples 5 times through 200 nm polycarbonate filter and 6 times through 100 nm polycarbonate filter (Nuclepore Track-Etched membranes, Whatman®, UK).

The purification was carried out by ultracentrifugation at 43000 rpm, 4 °C for 2 hours (Rotor 100.4 Ti, Beckman Ultracentrifuge, USA). The supernatant was further purified by ultrafiltration using Amicon®-Ultra-4 filter devices having molecular cut-off of 50 KDa (Merck Millipore Ltd. – Irland). At the end of the ultrafiltration process the formulation remaining on the filter was recovered and re-suspended in pure water, after have being washed three times with Milli-Q® water to assure the complete removal of the free drug. Conventional empty liposomes (CL) composed of 100% lipids (without surfactant) were prepared according to the same method (Table 1).

Table 1- Qualitative and quantitative (% w/w) composition of flexible liposomes.

FORMULATION	DOTAP	GLUTARYL-PE	TWEEN 80	UFH	EN	ND
F (-)	84	1	15	-	-	-
F1	84	1	15	0.5*	-	
F2	84	1	15	-	0.5*	
F3	84	1	15	-	-	0.5*
F4	84	1	15	1*	-	-
F5	84	1	15	-	1*	-
F6	84	1	15	-	-	1*
CL	98.82	1.18	-	-	-	-

* *mg/mL;* UFH: sodium unfractionated heparin; EN: enoxaparin; ND: nadroparin; CL: conventional empty liposomes

Physicochemical characterization of liposomes

The particle size distribution and ζ-potential of prepared liposomes were assessed by dynamic light scattering (DLS) using a Zetasizer (Nano-ZS, Malvern Instrument, UK). For particle size measurement, samples were introduced into a disposable cuvette after 10-fold dilution in Milli-Q® water, and the analysis was performed at the detection angle of 173°. For ζ-potential determination, the liposome suspension was inserted into a capillary cell after 1:10 dilution in 10 mM NaCl solution.

The mean diameter, the polydispersity index (PdI) and the ζ-potential of the carriers were measured within 0 and 6 months after storage under nitrogen atmosphere and in the dark at 4 °C, to assess the physical stability of liposomes.

The amount of drug carried by flexible liposomes was assessed by the carbazole assay[17]. Briefly, 200 µL of liposome samples were diluted up to 1 mL with Milli-Q® water. To each tube containing 1 mL sample, 5 mL of 25 mM solution of sodium tetraborate decahydrate in sulfuric acid 96% w/v were added. After vigorous mixing, samples were heated at 100 °C for 10 minutes in a water bath, then cooled under running water to room temperature. Then, 200 µL of 0.125 % w/v carbazole solution in absolute ethanol was added and mixed to each sample and the tubes were heated at 100°C for 15 minutes. Once the temperature of the samples cooled, the absorbance of the colored samples was read at 530 nm using a UV-spectrophotometer (Lambda 25, PerkinElmer – USA) against Milli-Q® water (treated as the samples). To estimate the interference of lipids, plain liposomes were assessed in parallel and used as control.

The concentration of all drugs was estimated based on calibration curves built for each molecule in the range of concentration 15-500 µg/mL ($R^2 \geq 0.99$). The drug concentration assayed by the carbazole method represents the overall amount of drug, both encapsulated and bound on the surface of liposomes, since the treatment in strong acidic environment inevitably leads to the rupture of the vesicles. The concentration of the drug was normalized per that of DOTAP (estimated accordingly to the method reported in the following section), and the encapsulation efficiency was expressed as mol/mol, drug/lipid ratio.

ATR-FTIR analysis

ATR-FTIR spectra were recorded between 4,000 and 450 cm^{-1} (264 scan, resolution: 2 cm^{-1}) using a Spectrum™One spectrophotometer (Perkin-Elmer, USA), equipped with a diamond crystal mounted in an ATR cell (Perkin-Elmer, USA).

The spectrum was automatically corrected by the ATR correction function and analyzed by Origin Pro 2015 (Origin Lab, USA). The maximum absorbance of peaks was assigned by second derivative. Fourier self-deconvolution of the hidden peaks of the C=O stretching band at 1730 cm^{-1} was resolved by the second-order derivative with respect to the wavelength after smoothing with a Savitsky–Golay function[18].

DOTAP quantitative determination

- *Equipments*

Analysis was performed using a Thermo Fischer Surveyor LC system equipped with a quaternary pump, a Surveyor UV–VIS Diode Array programmable detector 6000 LP, a Surveyor autosampler, a vacuum degasser, and connected to a TSQ Quantum Triple Quadrupole Mass Spectrometer (Thermo Fisher Scientific, Spa – Rodano, Milan, Italy). Chromatographic separations were done by reverse phase elution with a Zorbax SB-C18 column (150mm×2.1mm i.d.; particle size 3.5 µm) (Agilent Technologies Italia S.p.a. - Cernusco sul Naviglio, Milan, Italy), kept at 25 ◦C. The mass spectrometer was equipped with an electrospray interface (ESI), which was operated in positive-ion mode, and controlled by the Xcalibur software (version 1.4).

- *Preparation of stock solutions, calibration standards and quality controls*

A stock solution of DOTAP 100 µg/ml in $CHCl_3$ was prepared and stored at -20° C for one month. The stock solution was diluted further with a mixture of IPA/methanol/$CHCl_3$ 4/2/1 (v/v/v) containing 7.5 mM ammonium formate to obtain working solutions. The 0.25 µg/ml working solution was analyzed by LC–MS/MS to ensure that the concentrations of the original solution were within the limits of the maximum established error (≤3%) and was used as QC sample. Calibration samples were prepared by diluting the stock solution with a 0.5 µg/ml IS solution (in IPA/methanol/$CHCl_3$ 4/2/1 (v/v/v) containing 7.5 ammonium formate) to provide the following final concentrations: 0.025, 0.05, 0.1, 0.25, 0.5 and 1 µg/ml. Each calibration and QC sample was processed as described in the sample preparation.

- *Sample preparation*

Flexible liposome formulations were analyzed after dilution with a 0.5 µg/ml IS solution (in IPA/methanol/$CHCl_3$ 4/2/1 (v/v/v) containing 7.5 mM ammonium formate).

Epidermis samples were dried, then accurately weighted and extracted twice with 2 ml CH_3OH under agitation for 30 min at 4°C. The extracts were then combined and dried under nitrogen, and the residue was dissolved in 200µl CH_3OH and then diluted using the 0.5µg/ml IS solution (in IPA/methanol/$CHCl_3$ 4/2/1

(v/v/v) containing 7.5 mM ammonium formate). The diluted sample was filtered through 0.45-µm nylon filters (Millex HV, PVDF membrane, 13 mm, MILLIPORE - Vimodrone, Milan, Italy) and the filtrate transferred to the autosampler vial insert (10 µl samples injected).

- *Chromatographic and mass spectrometric conditions*

Separations were done by gradient elution from 15% water–formic acid 0.1% (v/v) (A) to 100% CH_3OH–formic acid 0.1% (v/v) (B) in 16 min at a flow rate of 0.2 ml/min (injection volume 10µl); the composition of the eluent was then restored to 15% (A) within 1 min and the system was re-equilibrated for 7 min. The sample rack was maintained at 4 ◦C. ESI interface parameters (positive-ion mode) were set as such: middle position; capillary temperature 270 ◦C; spray voltage 4.0 kV. Nitrogen was used as nebulizing gas at the following pressure: sheath gas 30 psi; auxiliary gas 5 a.u.

MS conditions and tuning were performed by mixing the diluted stock solution of DOTAP (flow rate 10µl/min) through a T-connection, with the mobile phase maintained at a flow rate of 0.2 ml/min. The intensity of the [M +H]+ ions were monitored and adjusted to the maximum by using the Quantum Tune Master® software. Quantitations were performed in multiple reaction monitoring (MRM) mode at 2.00 kV multiplier voltage, and the following MRM transitions of $[M+H]^+$ precursor ions → product ions were selected for each analyte and the relative collision energies optimized by the Quantum Tune Master® software:

m/z 312.3 → 60.3 (collision energy, 37 eV) RCM104 (IS);

m/z 662.5 → 265.3 + 603.5 (collision energy, 35 eV) DOTAP.

The parameters influencing these transitions were optimized as follows: argon gas pressure in the collision Q2: 1.5 mbar; peak full width at half maximum (FWMH): 0.70m/z at Q1 and Q3; scan width for all MRM channels: 1m/z; scan rate (dwell time): 0.2 s/scan.

- *Assay validation*

Calibration standards were prepared and analyzed in duplicates in three independent runs. The calibration curves were constructed by weighted ($1/x^2$) least-square linear regression analysis of the peak area ratios of DOTAP to the IS against nominal analyte concentration. The lower limit of quantitation (LLOQ), determined as the lowest concentration with values for precision and accuracy within ±20% and a signal-to-noise (S/N) ratio of the peak areas ≥10, was found to be 0.025 µg/ml.

Intra- and inter-day precisions and accuracies of the method were determined by assaying five replicates of the QC sample in three separate analytical runs. The calculated coefficient of variation (CV%) and the relative error (RE%) were 1.15 and 2.97, respectively. The recovery of the analyte was optimized repeating extraction until the detected amount was found below the limit of detection, to ensure a complete extraction. The specificity of the assay was evaluated by comparison of LC–MS/MS chromatograms of analyte at the LLOQ to those of blank tissue sample in triplicate. The stability of the processed sample, including the resident time in the autosampler (12 h at 4 °C), and stock solutions stability (4 weeks at 4 °C) were determined in triplicates.

The mean values of the triplicate samples were compared to the initial condition for all the stability tests, and they all range from 95.8 to 105.5% of the initial value.

Morphological analysis

- *Transmission Electron Microscopy (TEM)*

An aliquot of 5 µl of each population was placed on formvar coated single slot grids. After 2 minutes the excess of aqueous solution was removed with filter paper. Grids were air dried, stained with 2% aqueous uranyl acetate for 7 minutes, washed in distilled water and observed under a Zeiss EM 10 electron microscope (Gottingen, Germany) at 80 kV.

- *Atomic Force Microscopy (AFM)*

The topographical maps of the different liposome formulations have been acquired using a Bioscope Catalyst AFM (Bruker) operated in Peak Force Tapping (PFT) mode, in fluid. The sample preparation protocol has been optimized in order to preserve the liposomes intact upon adsorption on the imaging substrate, avoiding vesicle fusion and the formation of supported lipid bilayers[19]. To this purpose, 200 µl droplet of diluted solutions (below 0.02 mg/ml in 10mM NaCl buffer) of cationic liposomes, previously ultrafiltrated through Amicon filters (cut-off at 50 kDa), have been deposited onto negatively charged ruby-muscovite mica disks at room-temperature. Mica disks were glued onto larger Teflon disks, in order to spatially confine a small droplet of imaging buffer. Liposomes were allowed to adsorb onto mica for 4 minutes, then, after gentle washing with the imaging buffer, a new droplet of the same buffer was added and the sample was imaged. Typically, the scan area was 5 µm x 5µm, the image resolution was 512x512 points, the maximum applied force was 200-400 pN, and the ramp frequency and size were 1 kHz and 100 nm, respectively. Typical scan rate was 0.2 Hz. ScanAsyst Fluid cantilevers (Bruker) with force constant k = 1.2 N/m (calibrated by the thermal noise method[20] and tip with radius of 20 nm, have been used for the topographical/mechanical analysis. By means of the quantitative mechanical property mapping modulus (PF-QNM), PFT also provided, simultaneously to the topographic maps, the corresponding maps of the effective modulus of elasticity (Young's modulus) of liposomes, as described below and shown in Figure 3. Raw images have been flattened by typically subtracting line-by-line 1st-order polynomials to account for the local sample tilt. As the liposomes are deformed during the acquisition of the image, the deformation map calculated by the PF-QNM module has been summed to each topographic map in order to obtain the uncompressed topographies. Assuming constant volume of vesicles, in solution as well as upon adsorption on mica, we have calculated the effective diameters of vesicles as twice the radii of spheres having volumes equal to those of vesicles in uncompressed AFM topographies.

Determination of the deformability properties of liposomes

- *Extrusion assay*

Prior of the test, all the populations were diluted to have the same lipid concentration and the same particle count, as assessed by DLS analysis[21].

The extrusion assay was performed in compression mode using a dynamometer (INSTRON® 5965, ITW Test and Measurement Italia S.r.l – Italia). A gas-tight syringe was filled with 1 mL of diluted liposome suspension and inserted into the extruder casing fixed to a vertical holder, with the needle faced downwards and the plunger end in contact with a 50 N loading cell. The steel probe was put in contact with the syringe plunger that was moved at a constant speed of 1 mm/s, forcing the vesicle suspension to pass through the 50 nm polycarbonate membrane inside the extruder casing. To minimize the dead volume, before each test the membrane was pre-treated with 1 mL of pure water, which was extruded at the same rate.

The loading force (N) required to displace the plunger was measured and plotted as a function of plunger displacement (mm). The constant of deformability (k, N/mm) was derived from the slop of such curve. The registered force values were normalized by dividing them for the cross sectional area of the syringe to have the stress values, expressed in MPa, which were plotted as function of the plunger displacement to calculate the resistance opposed to deformation (σ).

At the end of the experiment, the extruded suspension was accurately weighed. The particle size of the vesicles was assessed before and after extrusion to calculate the percentage variation of liposome diameter (Δd_H), according to the following equation:

$$\Delta d_H = \frac{(\boldsymbol{R_{vi}} - \boldsymbol{R_{ve}})}{\boldsymbol{R_{vi}}} \boldsymbol{X\ 100}$$

where R_{vi} is the diameter of the vesicles before the experiment and R_{ve} represents the vesicle diameter after extrusion. Each formulation was extruded one time through the 50 nm polycarbonate membrane and each result is the mean of at least three determinations.

- *Nanomechanical analysis by AFM*

PF-QNM allows the acquisition of the topographic map and simultaneously the quantitative Young's modulus map of the sample. A force vs distance curve is recorded in each point of a grid spanning the area under investigation[22]. The piezo displacement at the force setpoint is recorded and used to calculate the local relative height of the sample (i.e. a point in the compressed topographic map); real-time analysis of the force curve provides the value of the local effective Young's modulus (i.e. a point in the elasticity map) and of the local indentation at the force setpoint. The indentation map is added to the compressed topographic map, to obtain the true topographic map. Here we have used the Derjaguin, Muller and Toporov (DMT) model of

contact mechanics: $F = \frac{4}{3} E\sqrt{R\delta^3} + F_{adh}$, where F is the applied force, Fadh is the adhesion force, E is the Young's modulus, R is the tip radius, and δ is the elastic indentation of the sample[23]. The analysis of the nanomechanical data is described in more details in the Supp. Info.

***In vitro* skin penetration studies**

*In vit*ro penetration studies were carried out using Franz diffusion cell method and human skin as a membrane. Skin samples were obtained by female healthy volunteers who underwent abdominoplasty and signed an informed consent for the use of the tissue for research purposes. Samples used in the experiments were prepared according to an internal protocol[8]. On arrival in the laboratory, the excess fat is carefully removed and full-thickness skin is cut into squares that are sealed in evacuated plastic bags and frozen at -20 °C until their use which occurred within one month. Epidermis sheets are obtained for gentle separation of epidermis from the remaining tissue with forceps, after skin immersion in water at 60 ± 1°C for 1 min. Prior to the experiment, the integrity of the tissue is assessed by measuring the electrical impedance of the epidermis sheets (voltage: 100 mV, frequency: 100 Hz; Agilent 4263B LCR Meter, Microlease, Italy). Only samples with values above 40 kΩcm^2 are used for the test[24].

Modified Franz diffusion cells having a wider column than the original Franz-type cell were used in the study. Each cell has a diffusion area of 0.636 cm^2 and a receiver compartment volume of about 3 mL. The human epidermis sheets were mounted on the lower half of the Franz diffusion cells with the stratum corneum facing upwards. The upper and lower parts of the cell were sealed with parafilm and fastened together with a clamp. The receiver compartment was filled with a 0.9 % w/v NaCl solution containing 100 µg/mL sodium azide as a preservative, and continuously stirred by a magnetic bar. 300 µL of liposome suspension were loaded in the donor compartment under non-occlusive conditions. The system was kept at 37 ± 1 °C by means of a circulating water bath so that the epidermis surface temperature was at 32 ± 1 °C throughout the experiment.

After 24 hours, the liposome suspensions were recovered from the donor compartment and assessed for particle size distribution by DLS. The epidermis sheets were dismounted from the cells, the formulation residues were removed with a cotton swab prior to wash the samples with 10 mL of milliQ® water. Afterwards, the epidermis sheets were cut into pieces of 2 cm^2 which were stripped with one tape (Transpore® tape, 3M, USA) to remove the superficial stratum corneum layers accordingly to an internal standard procedure[25]. Epidermis samples were let to dry and precisely weighted. The DOTAP retained in the epidermis was extracted and quantified according to the protocol reported above (sample preparation).

The penetration pattern of flexible liposomes was studied by TEM. For this test, human full-thickness skin was mounted on Franz diffusion cells with the stratum corneum facing the donor compartment, which was filled with 300 µL of liposome suspensions. The experiment was carried out accordingly to the protocol

described above. At the end of the test, the excess formulation was recovered from the donor compartment and the skin was cleaned with a cotton swab and washed with milliQ® water. Samples of 0.2 cm^2 were cut and immersed in phosphate buffer at pH 7.4 in a 6 multi-wells plate. Each sample was then fixed overnight at 4 C° in a solution containing 2% paraformaldehyde, 2% glutaraldehyde in cacodylate buffer, pH 7.3. Subsequently samples were post-fixed in 2% OsO_4, washed in distilled water, stained en bloc with 2% aqueous uranyl acetate, dehydrated through a series of acetones and embedded in Epon-Araldite resin. Ultra-thin sections, 60 nm thick, were cut with a diamond knife, using a Leica-Reichert Ultrotome SuperNova. Sections obtained from each sample were collected on formvar coated single slot grids, counterstained with lead citrate and examined with a Zeiss EM 10 electron microscope.

Statistical analysis

The comparison among the samples was performed by analysis of the variance followed by Bonferroni post-analyses (Daniel's XL Toolbox 5.06). The level of significance was taken as $p< 0.05$.

Results and discussion

Physicochemical and technological characterization of flexible liposomes

All cationic flexible liposome suspensions, after being purified by ultracentrifugation, showed the coexistence of two populations of vesicles, one appeared as a supernatant dispersed in the medium (Fs), as occurred in the case of plain liposomes, and one precipitated as a pellet (Fp). The two populations of liposomes were separated regardless of the speed (10000 or 100000g) and time of centrifugation (1, 2 or 5 hours). The free drug was removed from the population of supernatant by ultrafiltration.

The formation of two populations of vesicles in DOTAP liposomes was due to a different distribution of the heparins in the vesicles, which determines a variation of liposome's density. Indeed, regardless of the chemical features of the molecule, encapsulated heparin (mol drug/mol DOTAP) was found to be at least 2.7 fold higher for Fp than Fs (Table 1). Moreover, by increasing the drug concentration in the hydration medium up to 1 mg/mL, the saturation limit was probably reached and the separation of a third phase as a powder non re-dispersible in water was observed. The ATR-FTIR spectra confirmed that the precipitated powder is a complex between the excess of DOTAP and drug not encapsulated during vesicle formation. As represented in Figure 1, which reports the spectrum of the precipitate isolated after the preparation of formulation 4 in comparison with those of raw DOTAP and UFH, the signals related to the cationic lipid prevailed accordingly to the relative ratio of the two components. However, some bands clearly due to UFH are evident.

The main bands attributed to UFH in the 900-1000 cm^{-1} region significantly shift towards higher wavenumbers (980 cm^{-1}→1010 cm^{-1}; 1020 cm^{-1}→1030 cm^{-1}; 1050 cm^{-1}→1060 cm^{-1}). These variations are associated to a slight modification of the band at around 1730 cm^{-1} due to the stretching of the DOTAP – C=O moieties. The

second derivative of this band followed by deconvolution revealed the presence of two hidden peaks due to the two ester groups of DOTAP (1743 cm^{-1}; 1723 cm^{-1}) which were still detectable also in the spectra of the precipitated complex even if they slightly shifted towards higher wavenumbers (1745 cm^{-1}; 1725 cm^{-1}). These modifications along with the very significant depression of the band at about 3200 cm^{-1} suggested that the interactions among DOTAP and heparins might also occur via H-bonds other than electrostatic interactions.

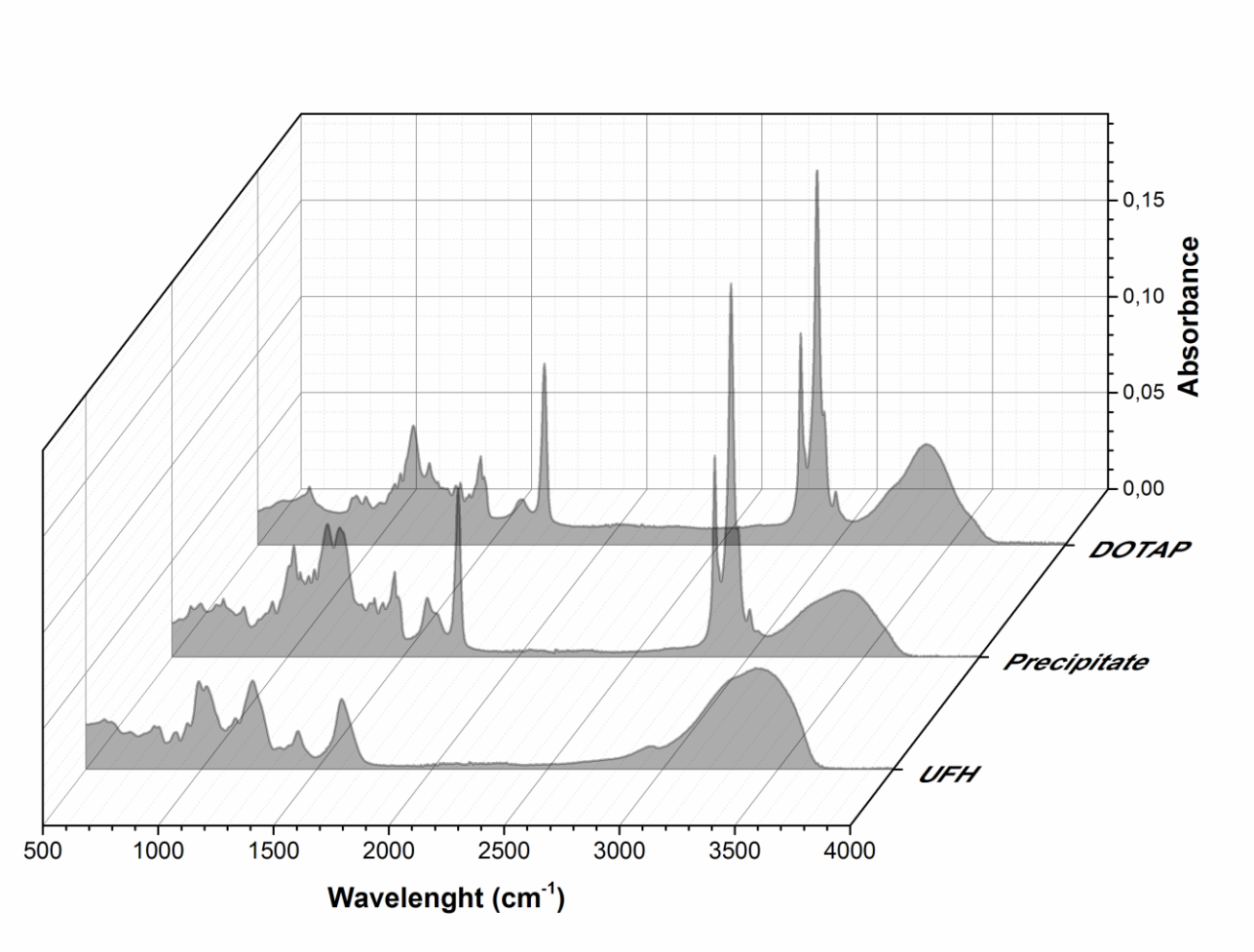

Figure 1 - ATR-FTIR spectra of raw DOTAP, UFH, and the precipitate isolated after the preparation of formulation 4.

Since the amount of precipitate was relevant and the encapsulation efficiency resulted very poor, formulations nos 4-6 were not considered for any further investigation.

Table 2 reports the main physicochemical and technological properties of all formulations and populations in study. All the populations were monodisperse (the polydispersity index, PdI, was lower than 0.1 in all cases) and the mean diameter of the vesicles (d_H) was always comprised within 100 and 200 nm, therefore suitable for the administration on the skin.

In the case of formulations prepared using the two low molecular weight heparins (LMWHs), the Fp populations had a larger d_H and a less positive ζ-potential compared to the plain liposomes (F(-)) and the

corresponding Fs populations (Table 2), thus suggesting the presence of a higher amount of drug adsorbed on the surface of these vesicles, as also supported by the TEM images (Figure 2). The only noticeable difference concerns the drug loading of the two Fp populations. Indeed, the ζ-potential values of F2p and F3p overlapped while the drug/DOTAP ratio resulted about 20% higher for F3p population (Table 2) suggesting that the stiffer structure of nadroparin, due to the complexation with calcium ions[8], allowed a better encapsulation in the aqueous core of the vesicle with respect to the enoxaparin having a very similar molecular weight.

In the case of UFH liposomes, the ζ-potential of the two populations, namely F1s and F1p, was not significantly different suggesting a different distribution of the glycosaminoglycan in the vesicles with respect to the two LMWHs. This may be explained by the higher affinity of UFH to DOTAP owing to the higher charge density and molecular weight with respect to enoxaparin and nadroparin[14], which may favour the distribution of UFH on the surface of the vesicles rather than in the aqueous core. In fact F1s showed the lowest ζ-potential combined to the lowest drug/lipid ratio among all Fs populations in study.

Table 2-Main physicochemical and technological parameters of flexible liposomes formulations.

Form.	Population	d_H (nm)	PdI	ζ (mV)	Carried drug (nM)	drug/ DOTAP (Mol/Mol x 10^3)
F(-)*	-	122.6 ± 15.6	0.09 ± 0.04	+ 50.6 ± 3.1	-	-
CL**	-	134.9 ± 3.46	0.09 ± 0.02	+ 56.0 ± 5.9	-	-
F1**	Fs	129.6 ± 2.1	0.08 ± 0.01	+ 42.2 ± 1.9	6.5 ± 0.1	0.41
(UFH)	Fp	185.2 ± 2.9	0.08 ± 0.02	+ 40.2 ± 2.3	8.9 ± 0.4	3.08
F2**	Fs	131.7 ± 6.6	0.09 ± 0.02	+ 47.7 ± 2.6	2.5 ± 0.5	1.13
(EN)	Fp	193.4 ± 3.8	0.12 ± 0.03	+ 44.4 ± 5.5	10.4 ± 3.0	3.09
F3**	Fs	125.6 ± 5.9	0.09 ± 0.03	+ 47.1 ± 1.9	3.1 ± 0.7	1.27
(ND)	Fp	183.4 ± 2.8	0.10 ± 0.03	+ 40.7 ± 5.2	13.2 ± 4.5	3.50

d_H: mean diameter determined by DLS; UFH: Unfractionated heparin; ND: nadroparin; EN: enoxaparin; CL: conventional empty liposomes; * n= 6; ** n= 3.

The monitoring of the particle size and ζ-potential of the formulations of cationic liposomes over 2 months' time did not reveal any significant variation of the mean physicochemical properties of the lipid vesicles, confirming the stability of the formulations when stored at 4 °C (Supporting info, Figure S1).

Morphological analysis

The morphological analysis demonstrated that both populations of vesicles (Fs and Fp) are composed of unilamellar liposomes, whose diameters appeared larger than those measured by DLS because of the adsorption and negative stain when a drop of liposomes is placed directly on the covered grids. TEM images showed the presence of almost spherical vesicles having an electron-dense core, consistent with the presence of the drug inside the vesicles (Figure 2). The electron-density of heparins avoided the detection of the lipid bilayer of vesicles whereas it was revealed a pale and thin shell surrounding the aqueous core of liposomes, probably the index of the drug absorbed on the surface of the carrier. This shell has net and regular edges in the case of Fs vesicles. Fp vesicles present instead a more irregular and expanded halo, particularly the F2p ones, as evidenced by high-magnification TEM images.

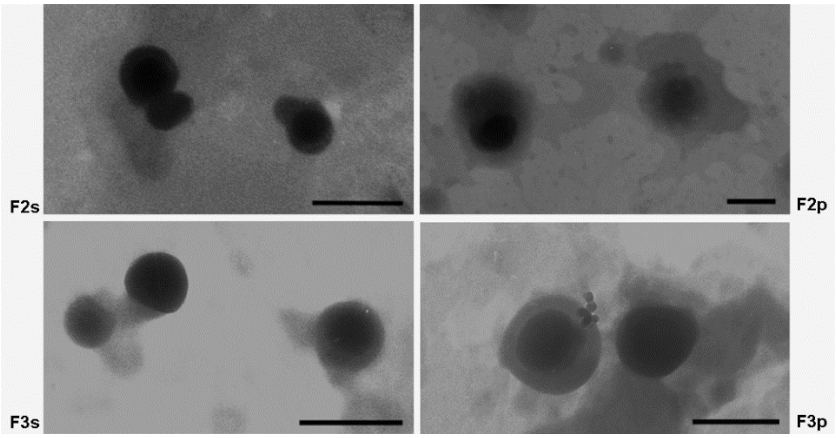

Figure 2- TEM images of cationic flexible liposome populations containing low molecular weight heparins (enoxaparin, namely F2s and F2p, and nadroparin, namely F3s and F3p). Fs and Fp are the vesicle population distributed in the supernatant and in the pellet respectively, after ultracentrifugation. The scale bar is equal to 300 nm.

The morphology evidenced by TEM was in agreement with AFM imaging. As shown in Figure 3 (left column), AFM images demonstrated that liposomes, once adhered on a solid surface, flatten assuming to a good approximation the shape of spherical caps, which is typical of collapsed spheroidal vesicles when they move from the bulk solution to a smooth two-dimensional surface[26]. The size of the vesicle as measured by deformation-corrected AFM topographies (under the assumption of constant volume) is typically in good agreement with the average DLS results in the case of the control formulation F(-) and the supernatant populations; in the case of the pellet, smaller values are found, although within the low-values tail of the DLS diameter distribution. Under optimal sample preparation conditions it is possible to perform a combined topographical and nanomechanical analysis of lipid vesicles, since vesicles appear well separated on the mica surface and stable upon repeated tip scanning at moderate loads, providing the quantitative map of the

effective Young's modulus of the vesicles in one-to-one correspondence to the topographic map (Figure 3, right column).

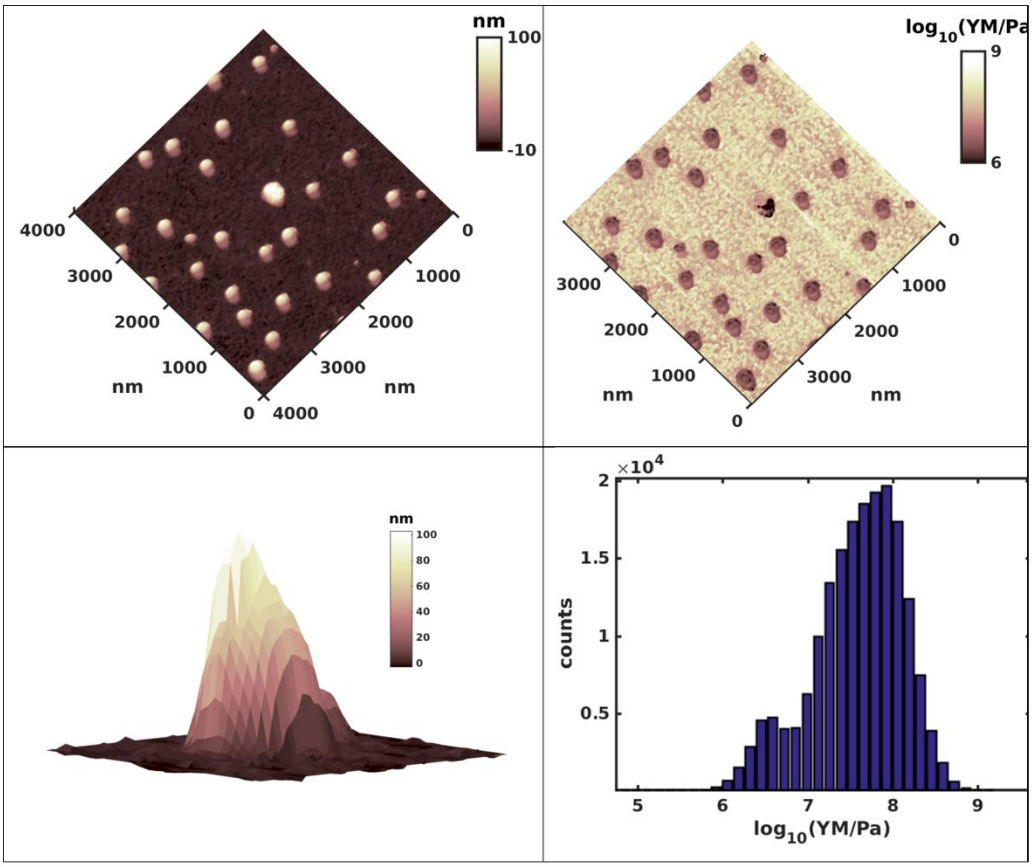

Figure 3- Top: representative coupled AFM topographic and Young's modulus maps of cationic flexible liposomes containing heparin (formulation F1, supernatant) deposited on mica and imaged in 10 mM NaCl solution. Bottom: on the left, a single liposome at higher magnification (image size: 500nm x 500nm); on the right, the distribution of YM values extracted from the elasticity map.

Deformability properties of flexible cationic liposomes

The most widely used approach to evidence liposome deformability relies on the extrusion under a constant and well defined pressure (ΔP ≥ 0.5 MPa) of the vesicle suspension through semipermeable membranes with small pores (generally 30-50 nm)[7]. The basic principle is that conventional liposomes, having a stiff bilayer, in most cases undergo fragmentation occluding the tiny pores of the membrane whereas flexible liposomes, being deformable, pass through the membrane maintaining their morphology and undergoing little variation of particle size after extrusion[27]. In such pressure-governed process, the flux (the amount of suspension extruded in a fixed time lap) is proportional to the relative vesicle/pore radii ratio and then the deformability can be calculated according to two different equations reported by Van der Bergh at al. and Manca et al[28-29].

Using similar experimental conditions, other authors proposed a simpler approach consisting in the expression of deformability as the reduction of vesicle diameters after extrusion[30].

In our approach, the test was performed at a constant rate to monitor the variation of the forces during the whole extrusion process, rather than measuring indirect and *ex post* parameters (i.e. weight/volume of the extruded suspension over time and/or particle size reduction).

Figure 4 reports the representative stress-displacement curves registered during the extrusion of liposome suspensions at a constant rate. In general, the curve can be divided in three different sections: first, the curve rapidly rises overcoming the initial friction associated to the displacement of the syringe plunger (A); then it continues to grow up to a second peak (B), eventually reaching a plateau, or linearly increasing until the end of the experiment (C).

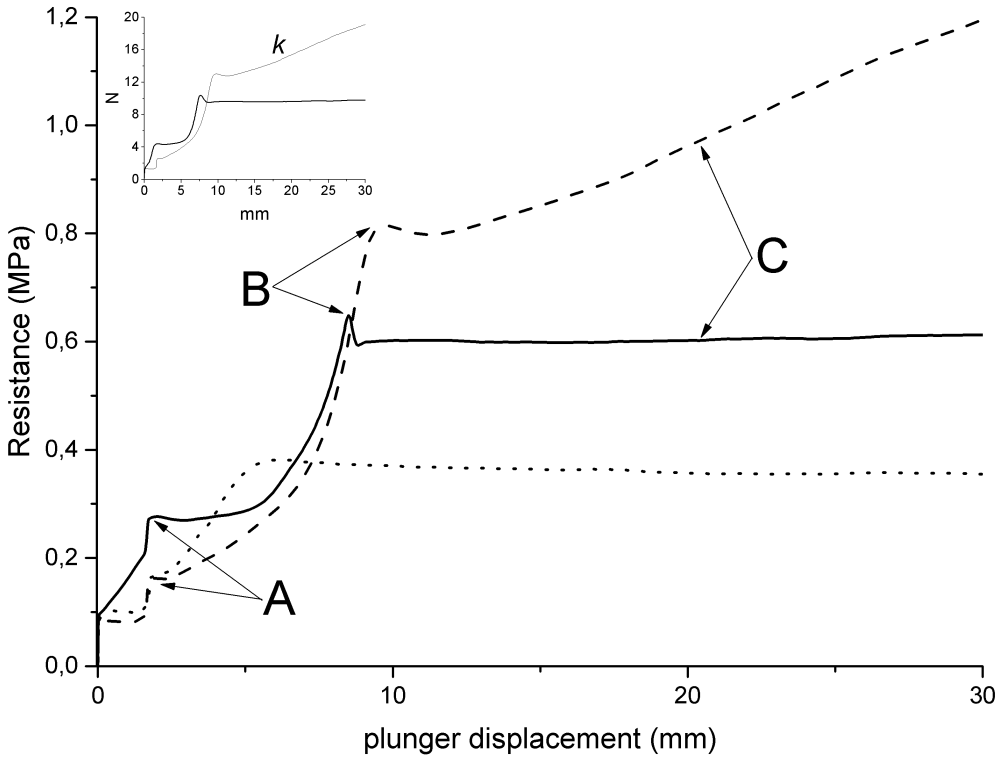

Figure 4 - Representative stress-displacement curves of flexible cationic liposomes as obtained by the extrusion assay developed using the dynamometer. The smaller panel reports the force (N)-displacement (mm) curve used to calculate the constant of deformability, K. In the figure, the black solid line refers to the plain flexible liposomes (F(-)), whereas the dashed line describes the behaviour of conventional liposomes and dotted line that of pure water.

In the case of the designed flexible plain liposomes (F(-)), the curve shape can be explained as follows. When lipid-surfactant mixed vesicles undergo an anisotropic stress (during the penetration in narrow pores), an initial activation energy is required for bilayer bending (peak B, Figure 4). This energetic cost is proportional

to the surface area of the vesicles and to the bending modulus[31]. Afterwards, the bilayer of the vesicles undergoes a structural rearrangement with the surfactant, which has affinity for curved conformations, relocated in the zones of maximum stress whereas the lipids enrich the others[6]. As a consequence of this structural rearrangement, vesicles modify spontaneously their shape (from spherical to ellipsoidal) for equal volume, thus flattening into the pores. The resistance opposed to this deformation (σ) is then dependent on the intrinsic characteristics of the vesicles in terms of bilayer rigidity and was identified in the peak B of the curve. Afterwards, the resistance decreases becoming almost constant and the registered values provide an indication of the force that is necessary to move the vesicles through the channel of the membrane.

In the case of conventional liposomes, the bending rigidity is high due to the lack of a natural curvature of the bilayer, therefore the energy required for the bilayer bending, and consequently σ, is higher than that of flexible liposomes[32](Figure 4). Moreover, in the region C, the force continues to increase linearly and this pattern was attributed to the progressive fragmentation of the vesicles in the pores. Therefore, two different parameters can be derived from the curves: the resistance to the initial deformation, σ, which is related to the activation energy for bilayer bending deformation; and the constant of deformability (K), calculated from the slope of the linear region of the force-displacement curve (insert of Figure 4), which provides an indication of the ability of the vesicles to flatten and permeate through the tiny pores of the membrane. Accordingly, the K value shifted from 0.295 ± 0.06 N/mm to 0.015± 0.003 N/mm passing from conventional liposomes to plain flexible liposomes (F(-)).

Basing on the previous considerations, it may be assumed that, among a set of formulations and for equal experimental conditions, flexible vesicles exhibit K values that tend to zero and low σ values, as result of a decreased bilayer rigidity.

The loading of LMWHs affected the flexibility of the liposome bilayer, in an extent dependent on the drug/lipid ratio and on the different distribution of the drug within the vesicles of Fs and Fp populations (see above). Indeed, σ increased in the following rank order: F(-) < Fs < Fp (Table 2). The K seemed particularly affected by the drug loading as can be observed comparing the values obtained with the LMWHs Fp vesicles. In fact, the K registered for F3p resulted significantly larger than that determined for the F2p population (Table 3) accordingly to the higher amount of drug encapsulated in the core, which would obstacle the shape change required for deformation when the vesicles undergo compression forces and/or a partial obstruction of the pores as in the case of CL formulation.

The F1s/F1p pair had similar σ and k values. F1s is quite similar to the other two Fs population even though the drug/DOTAP ratio is half and the ζ potential was significantly lower. The F1p resulted more flexible than the other two Fp populations even if the drug/DOTAP ratio and the ζ potential were very close to that of enoxaparin. The reasons of this different behaviour were not completely understood and their clarification should require a specific study that is out of the scope of this work. However, it may be ascribed to the higher average Mw and charge of UFH with respect to enoxaparin and nadroparin, which determined a different

rearrangement of the macromolecule on the liposome surface, thus altering in lower extent the capability of the vesicles to adapt in ellipsoidal structures during the pore penetration.

At the end of the experiments the percentage of reduction of vesicle diameters (Δd_H) was also calculated. The Δd_H values found for all populations were low and in a range according to the data reported in literature for flexible liposomes[30;33]. However, the trend did not result related to any physicochemical property of liposomes, suggesting the unsuitability of this approach when the experiments are performed at constant rate (Table 3).

Table 3- Elastic properties of flexible cationic liposomes.

F	P	Δd_H	σ (MPa)	K (N/mm)	Log_{10}(YM) (Pa)
F(-)*	-	16.25 ± 1.10	0.65 ± 0.10	0.015 ± 0.003	6.19 ± 0.09
F1	**Fs**	13.9 ± 2.27	1.16 ± 0.09	0.050 ± 0.012	6.47 ± 0.09
	Fp	12.01 ± 2.00	1.43 ± 0.10	0.065 ± 0.013	7.04 ± 0.10
F2	**Fs**	13.68 ± 2.99	0.95 ± 0.04	0.044 ± 0.007	6.43 ± 0.24
	Fp	21.41 ± 0.50	1.89 ± 0.30	0.125 ± 0.025	7.19 ± 0.21*
F3	**Fs**	15.63 ± 0.20	0.80 ± 0.08	0.038 ± 0.008	6.36 ± 0.10
	Fp	11.65 ± 1.15	1.75 ± 0.19	0.195 ± 0.042	7.27 ± 0.16*

*Not statistically different, p> 0.5

Since the mechanical parameters derived from the dynamometer extrusion method are not absolute parameters, the results obtained with this approach were compared to those of the effective Young's modulus (log_{10}(YM)) of single vesicles obtained by AFM nano-indentation tests. AFM analyses were performed in parallel since this technique has been widely employed for the topographic, physicochemical and technological analysis of lipid layers and liposomes [26, 34-35] and can effectively and accurately characterize the elastomechanical properties of nanoscale vesicles[36].

It was observed that the log_{10}(YM) calculated by AFM followed the same trend of the resistance registered during the extrusion of the prepared liposomes suspensions, being higher for Fp populations than the corresponding Fs populations and F(-) (Table 3). Moreover, the AFM data confirmed the relevance of the mean diameter of the vesicles in determining the vesicle deformability. Indeed, the larger the mean diameter, the higher the log_{10}(YM). This result can be explained considering that the elongation factor (i.e. the ratio between the length of a deformed vesicle in a pore and the diameter of the original spherical vesicle) increases as the vesicles radius increases, and the larger the elongation factor, the higher is the energetic cost for vesicle elongation in the pore[37]. Accordingly, F2p, showed the lowest deformability (highest σ, highest log_{10}(YM)) among all the populations of vesicles analysed (Table 1). It is important to highlight that

the $\log_{10}$(YM) determined by AFM were in good correlation with the σ values calculated during the vesicle extrusion (F=71.52, Adj R^2=0.9216, Figure 5). This was expected since both parameters strongly depend on the intrinsic rigidity of the bilayer rather than on the conformational change of the vesicles, as is the case for the constant of deformability, k. Interestingly, for similar reasons, both σ and $\log_{10}$(YM) seem to be affected by the presence of drug on the surface, as attested by the fact that F1s, having the lowest ζ-potential values among the Fs populations, showed the highest σ and $\log_{10}$(YM) values. As further proof of this hypothesis, the comparison of F2p and F3p deformability values (Table 3) revealed that the larger amount of nadroparin in the liposome core did not influence σ and $\log_{10}$(YM) values as it does for k.

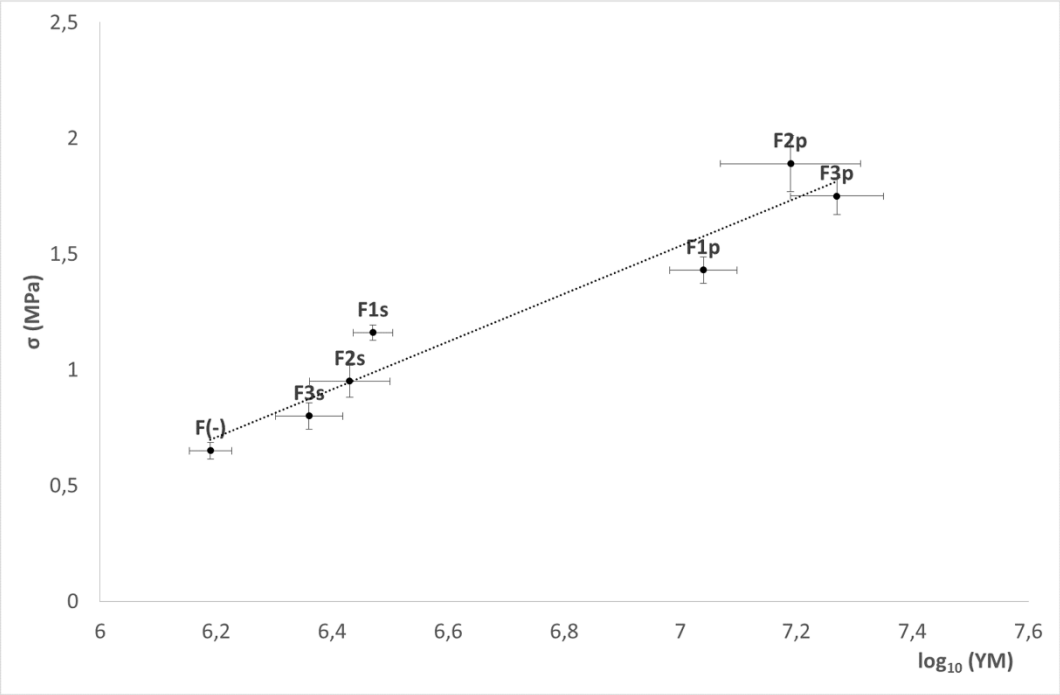

Figure 5- Correlation between σ and $\log_{10}$(YM) values of all formulations and populations in study as measured by dynamo-mechanical and AFM analyses (R^2=0.9347). The data are reported as mean ± standard error.

In vitro penetration studies

The in vitro assays were carried out using F(-) and formulations loaded with enoxaparin (F2s and F2p), since they covered all scale of elastic parameters (Table 3).

DLS analyses performed on the liposome suspensions recovered from the donor compartment at the end of the experiment did not evidence any fusion or aggregation of liposomes on the skin surface since the d_H and PdI of the liposome suspensions remained unchanged (data not shown). Only a decrease of the particles count was observed. Although a little amount of suspension was still found at the end of the experiment and therefore the liposomes did not completely dry on the skin surface, as it is assumed in non-occlusive

condition, the lipid suspension significantly concentrated on the skin surface. This caused the de-swelling of the vesicles, thus maintaining the gradient for enhancing their skin penetration[38].

TEM images taken on full-thickness skin samples after 24 hours exposure to liposomal formulations revealed the presence of intact vesicles in the deeper layers of the epidermis. In particular, after treatment with empty flexible liposomes (F(-)) and F2s, different groups of intact vesicles were found both in the stratum granulosum and spinosum of the epidermis (F(-), Figure 6), whereas in the skin samples treated with F2p population, few groups of vesicles were still observed, but they were confined to the stratum granulosum (Figure 7).

Our results are in line with those obtained by Subongkot and co-workers[39], who observed by TEM the penetration of intact vesicles in the viable epidermis of pig skin samples *in vitro,* even if in our case the treatment with liposomal formulations did not seem to alter the epidermis ultrastructure . It was noticed instead that the vesicles flowed together through preferential pathways since a massive presence of vesicles, partially even overlapped, was observed in certain regions of the tissue with respect to others. This phenomenon can be explained considering that flexible liposomes diffuse preferentially (if not exclusively) through the channel-like hydrophilic pores which are more abundant in correspondence of the lateral cell junction[6]. The hypothesis of a preferential diffusion in the channel-like regions of the stratum corneum was in agreement with freeze-fracture electron microscopy images recorded after *in vivo* tape stripping experiment[40].

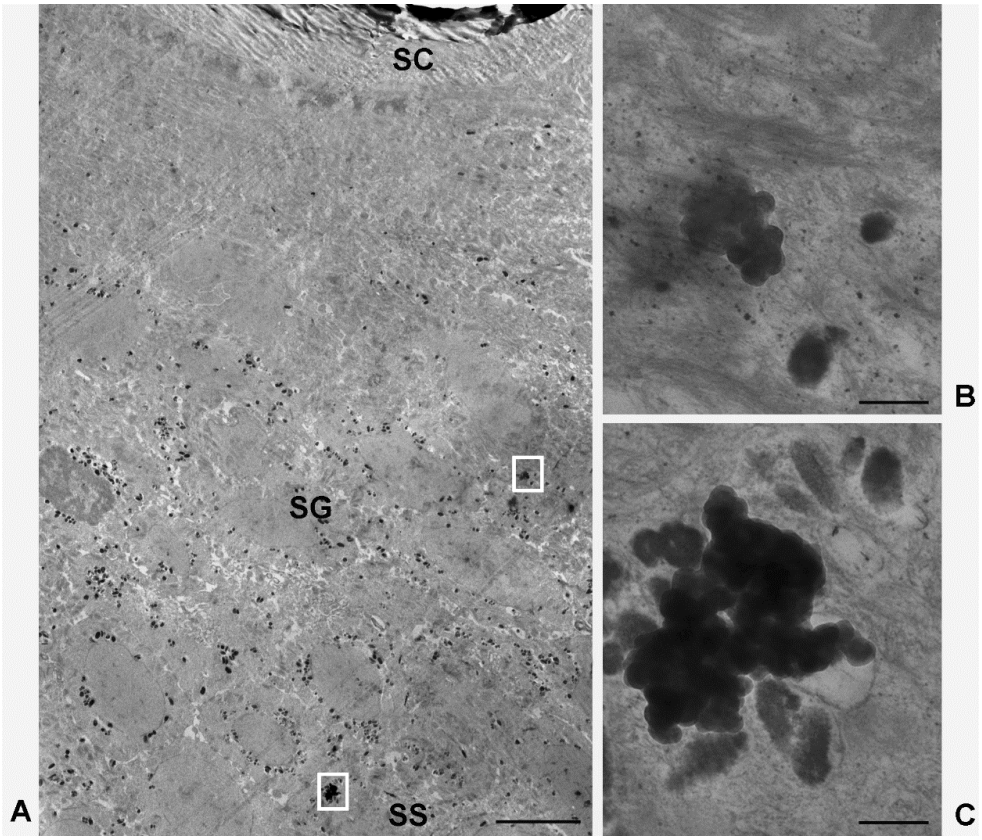

Figure 6- TEM image of human epidermis (A) exposed to the flexible cationic liposome formulation F(-). SC= stratum corneum; SG= stratum granulosum; SS= stratum spinosum, scale bar= 4 µm. Boxed areas enlarged in B and C show two groups of liposomes, scale bar= 200 nm.

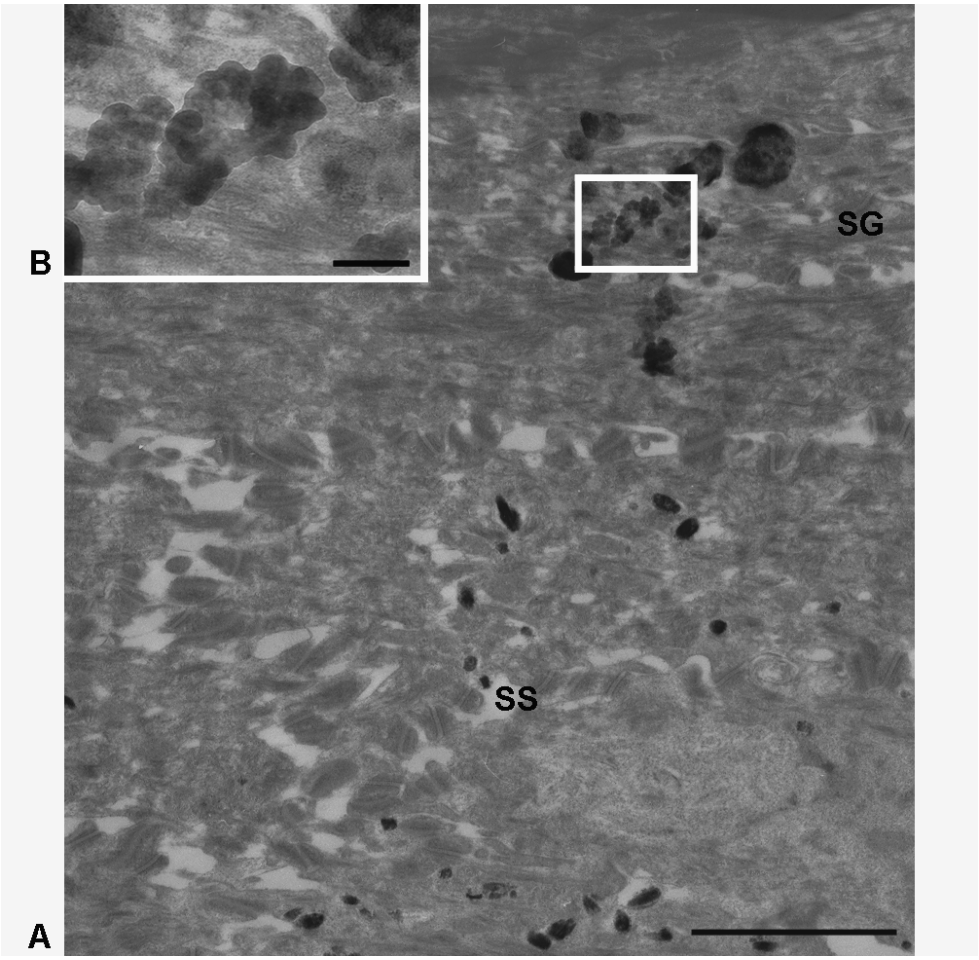

Figure 7- TEM image of human epidermis (A) exposed to the flexible cationic liposome population F2p. SG= stratum granulosum; SS= stratum spinosum, scale bar= 2 µm. Boxed area enlarged in B shows some vesicles partially overlapped, scale bar= 200 nm.

Basing on the evidences of these *in vitro* studies, the increase of the membrane rigidity caused by enoxaparin, then, did not completely prevent the penetration of the vesicles into the skin, but limited the depth of vesicles penetration.

Moreover, a relationship was found between the level of flexibility and the extent of penetration after 24h of exposure (R_{24}): the higher the flexibility (the lower the σ and K values), the higher the penetrated amount of DOTAP in the epidermis (Figure 8). In fact, the amount of DOTAP extracted from the tissue after 24 h exposure to flexible liposomes decreased, increasing the bilayer rigidity in the following rank order: F(-) (R_{24}= 3.33 ± 0.02 µg/mg) > F2s (R_{24}= 1.18 ± 0. 26 µg/mg)> F2p (R_{24}= 0.53 ± 0.33 µg/mg), confirming the relevance of elasticity on skin penetration properties of such carriers.

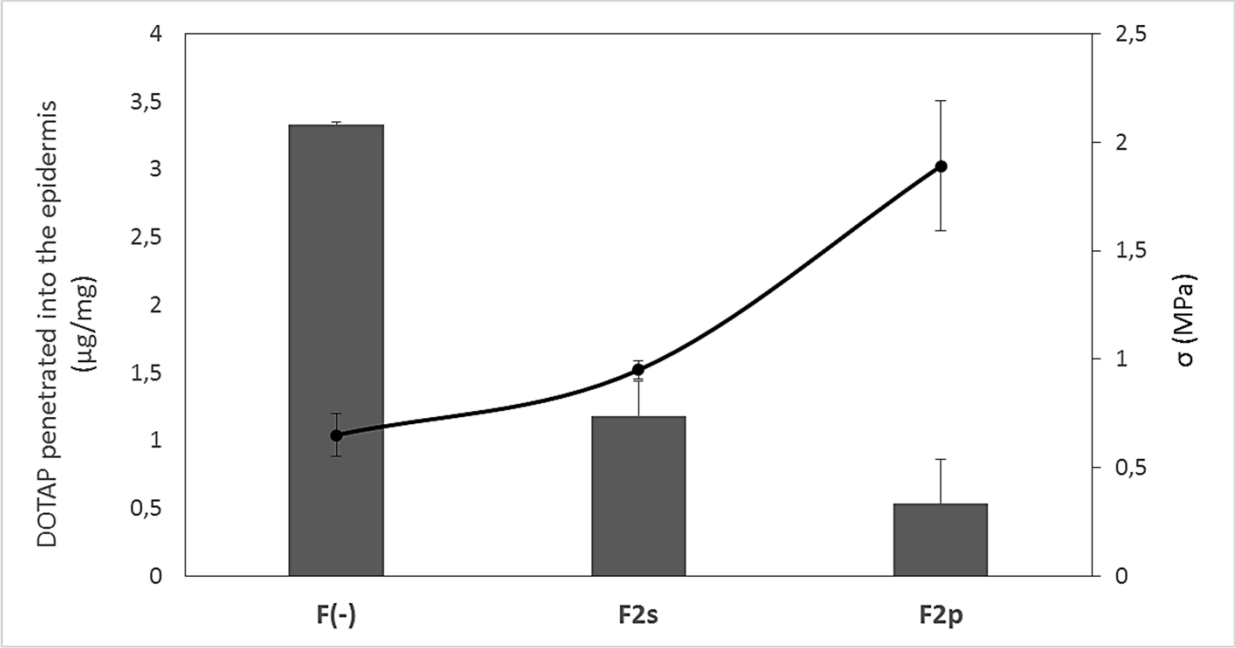

Figure 8- Penetrated amount of DOTAP in the deeper epidermis after 24 hours exposure to empty flexible liposomes, F(-), and the two population of vesicles containing EN, F2s and F2p, as quantified by HPLC-ESI-MS/MS method after removal of the superficial layers of the skin by tape-stripping.

Conclusions

Although the real mechanism and the forces involved in the skin penetration of flexible liposomes is highly debated and many details are still not completely understood, this work has demonstrated that the degree of flexibility of the lipid vesicles exerts a key role in determining both the extent and the depth of liposome penetration into human epidermis. Indeed, the increase of the liposome elastic modulus by heparins encapsulation drastically affected the ability of the vesicles of repartition among the epidermis layers. It should be noted, that this is the first work, to the best of our knowledge, in which whole vesicles were observed as such in biological tissues without further manipulation of the samples. Since changes in liposome composition and drug encapsulation can alter the rearrangement properties of the bilayer, which is the main requirement for the efficiency of such drug carriers, it is highly desirable to have methods suitable to assess the contribution of the formulation variables on liposome flexibility, which might be accurately tuned according to the final therapeutic target. The proposed dynamometer assisted extrusion method, following the forces involved in the different steps of vesicles deformation, allows determining the changes of fluidity of the liposome bilayer induced by drug loading. Indeed, the good correlation found between the parameters calculated with this method (the constant of deformability, K, and the resistance to the initial bilayer deformation, σ) and the elastic moduli derived from the topographic images registered by AFM, supports the

reliability of the novel approach, and might be proposed as a simple tool for monitoring the liposome flexibility at macroscale. Beside the characterization of liposomes intended for (trans)dermal delivery, this easy-to-perform test may be applied to the investigation of the fluidity of different liposomal formulations, facilitating the comprehension of the stability and release properties of liposomes developed for different purposes and routes of administration.

Conflict of Interest: The authors declare no competing financial interest.

Supporting Information Available: Additional information includes the stability of the liposomes over a period of 2 months (up to 6 months for the formulations used in the in vitro permeability assay), details of the nanomechanical analysis protocol, and representative LC-MS/MS chromatograms.

References:

1. Cevc, G. Lipid vesicles and other colloids as drug carriers on the skin. *Adv. Drug Delivery Rev*. **2004**, 56, 675–711.
2. Cevc, G.; Vierl, U. Nanotechnology and the transdermal route. A state of the art review and critical appraisal. *J. Controlled Release* **2010**, 141, 277–299.
3. González-Rodríguez, M.L.; Rabasco, A.M. Charged liposomes as carriers to enhance the permeation through the skin. *Expert Opin. Drug Delivery* **2011**, 8 (7), 857-871.
4. Elsayed, M.M.A.; Abdallah, O.Y.; Naggar, V.F.; Khalafallah, N.M. Lipid vesicles for skin delivery of drugs: Reviewing three decades of research. *Int. J. Pharm*. **2007**, 332, 1–16.
5. Campani, V.; Biondi, M.; Mayol, L.; Cilurzo, F.; Franzé, S.; Pitaro, M.; De Rosa, G. Nanocarriers to Enhance the Accumulation of Vitamin K1 into the Skin. *Pharma Res* **2016**, 33 (4), 893-908.
6. Morilla, M.J.; Romero, E.L. Carrier deformability in Drug Delivery. *Curr. Pharm. Des*. **2016**, 22, 1118-1134.
7. Cevc, G.; Gebauer, D.; Stieber, J.; Schätzlein, A.; Blume, G. Ultraflexible vesicles, Transfersomes, have an extremely low pore penetration resistance and transport therapeutic amounts of insulin across the intact mammalian skin. *Biochim. Biophys. Acta* **1998**, 1368, 201–215.
8. Franzé, S.; Gennari, C.G.M.; Minghetti, P.; Cilurzo, F. Influence of chemical and structural features of low molecular weight heparins (LMWHs) on skin penetration. *Int. J. Pharm*. 2015, 481(1–2), 79–83.
9. Boakye, C.H.A.; Patel, K.; Singh, M. Doxorubicin liposomes as an investigative model to study the skin permeation of nanocarriers. *Int. J. Pharm*. **2015**, 489, 106–116.
10. Hasanovic, A.; Hollick, C.; Fischinger, K.; Valenta, C.; Improvement in physicochemical parameters of DPPC liposomes and increase in skin permeation of aciclovir and minoxidil by the addition of cationic polymers. *Eur. J. Pharm. Biopharm*. **2010**, 75, 148–153.
11. Eun-kyung, O.; Su-Eon, J.; Jin-Ki, K.; Jeong-Sook, P.; Youmie, P.; Chong-Kook, K.; Retained topical delivery of 5-aminolevulinic acid using cationic ultradeformable liposomes for photodynamic therapy. *Eur. J. Pharm. Sci*. **2011**, 44, 149–157.
12. Ruponen, M.; Rönkkö, S.; Honkakoski, P.; Pelkonen, J.; Tammi, M.; Urtti, A. Extracellular Glycosaminoglycans Modify Cellular Trafficking of Lipoplexes and Polyplexes. *J. Biol. Chem.* **2001**, 36 (7), 33875-33880.
13. Nyren-Erickson, E.K.; Haldar, M.K.; Totzauer, J.R.; Ceglowski, R.; Patel, D.S.; Friesner, D.L.; Srivastava, D. K.; Mallik, S. Glycosaminoglycan-Mediated Selective Changes in the Aggregation States, Zeta Potentials, and Intrinsic Stability of Liposomes. *Langmuir* **2012**, 28, 16115−16125.
14. Minghetti, P.; Cilurzo, F.; Franzé, S.; Musazzi, U.M.; Itri, M. Low molecular weight heparins copies: are they considered to be generics or biosimilars? *Drug Discovery Today* **2013**, 18 (5-6), 305-311.

15. Perez, A.P; Altube, M.J; Schilrreff, P.; Apezteguia, G.; Santana Celes, F.; Zacchino, S.; Indiani de Oliveira, C.; Romero, E.L.; Morilla, M.J. Topical amphotericin B in ultradeformable liposomes: Formulation,skin penetration study, antifungal and antileishmanial activity in vitro. Colloids Surf., B **2016**, 139, 190–198.
16. El Zaafarany, G.M.; Awad, G.A.S.; Holayel, S.M.; Mortada, N.D. Role of edge activators and surface charge in developing ultradeformable vesicles with enhanced skin delivery. *Int. J. Pharm.* **2010**, 397 (1-2), 164-172.
17. Bitter, T.; Muir, H.M. A modified uronic acid carbazole reaction; *Anal Biochem* **1962**, 4, 330–334.
18. Gennari, C.G.M.; Franzè, S.; Pellegrino, S.; Corsini, E.; Vistoli, G.; Montanari, L.; Minghetti, P.; Cilurzo, F. Skin Penetrating Peptide as a Tool to Enhance the Permeation of Heparin through Human Epidermis. *Biomacromolecules* **2016**, 17, 46-55.
19. Jass, J.; Tjärnhage, T.; Puu, G. From Liposomes to Supported, Planar Bilayer Structures on Hydrophilic and Hydrophobic Surfaces: An Atomic Force Microscopy Study. *Biophys. J.* **2000**, 79(6) , 3153–3163.
20. Butt, H.J.; Cappella, B.; Kappl, M. Force measurements with the atomic force microscope: Technique, interpretation and applications. *Surf. Sci. Rep.* **2005**, 59, 1-152.
21. Shang, J; Gao, X. Nanoparticle Counting: Towards Accurate Determination of the Molar Concentration. *Chem Soc Rev.* **2014**, 43(21), 7267–7278.
22. Cappella, B.; Dietler, G. Force-distance curves by atomic force microscopy. *Surf. Sci. Rep*. **1999**, 34, 1-104.
23. Derjaguin, B.V.; Muller, V.M.; Toporov, Y.P. Effect of Contact Deformations on the Adhesion of Particles. *J. Colloid Interface Sci*. **1975**, 53 (2), 314-325.
24. Kasting, G.B.; Bowman, L.A. DC electrical properties of frozen, excised human skin. *Pharm Res*. **1990**, 7(2), 134-43.
25. Minghetti, P.; Casiraghi, A.; Cilurzo, F.; Montanari, L. Development of local patches containing melilot extract and ex vivo–in vivo evaluation of skin permeation. Eur J Pharm Biopharm 2000, 10, 111–117.
26. Schönherr, H.; Johnson, J.M.; Lenz, P.; Frank, C.W.; Boxer, S.G. Vesicle Adsorption and Lipid Bilayer Formation on Glass Studied by Atomic Force Microscopy. *Langmuir* **2004**, 20 (26), 11600–11606.
27. Ogunsola, O.A.; Kraeling, M.E.; Zhong, S.; Pochan, D.J.; Bronaughd, R.L.; Raghavan, S.R. Structural analysis of “flexible” liposome formulations: new insights into the skin-penetrating ability of soft nanostructures. *Soft Matter* **2012**, 8, 10226-10232.
28. Van den Bergh, B.A.; Wertz, P.W.; Junginger, H.E.; Bouwstra, J.A. Elasticity of vesicles assessed by electron spin resonance, electron microscopy and extrusion measurements. *Int. J. Pharm*. **2001**, 217, 13-24.

29. Manca, M.L.; Zaru, M.; Manconi, M.; Lai, F.; Valenti, D.; Sinico, C.; Fadda, A.M. Glycerosomes: a new tool for effective dermal and transdermal drug delivery. *Int J Pharm.* **2013,** 455, 66–74.
30. Geusens, B.; Lambert, J.; De Smedt, S.C.; Buyens, K.; Sanders, N.N.; Van Gele, M. Ultradeformable cationic liposomes for delivery of small interfering RNA (siRNA) into human primary melanocytes. *J. Controlled Release* **2009**, 133, 214–220.
31. Cevc, G.; Schätzlein, A.G.; Richardsen, H.; Vierl, U. Overcoming Semipermeable Barriers, Such as the Skin, with Ultradeformable Mixed Lipid Vesicles, Transferosomes, Liposomes, or Mixed Lipid Micelles. *Langmuir* **2003**, 19, 10753-10763.
32. Rawicz, W.; Olbrich, K.C.; McIntosh, T.; Needham, D.; Evans E. Effect of Chain Length and Unsaturation on Elasticity of Lipid Bilayers. *Biophys J*. **2000**, 79, 328–339.
33. Geusens, B.; Van Gele, M.; Braat, S.; De Smedt, S.C.; Stuart, M.C.A.; Prow, T.W.; Sanchez, W.; Roberts, M.S.; Sanders, N.N.; Lambert, J. Flexible Nanosomes (SECosomes) Enable Efficient siRNA Delivery in Cultured Primary Skin Cells and in the Viable Epidermis of Ex Vivo Human Skin. *Adv. Funct. Mater*. **2010**, 20, 4077–4090.
34. Alessandrini, A.; Facci, P. Nanoscale mechanical properties of lipid bilayers and their relevance in biomembrane organization and function. *Micron.* **2012**, 43(12), 1212-23.
35. Indrieri, M.; Suardi, M.; Podestà, A.; Ranucci, E.; Ferruti, P.; Milani, P. Quantitative Investigation by Atomic Force Microscopy of Supported Phospholipid Layers and Nanostructures on Cholesterol-Functionalized Glass Surfaces. *Langmuir* **2008**, 24(15), 7830–7841.
36. Takechi-Haraya, Y.; Sakai-Kato, K.; Abe, Y.; Kawanishi, T.; Okuda, H.; Goda, Y. Atomic Force Microscopic Analysis of the Effect of Lipid Composition on Liposome Membrane Rigidity. *Langmuir* **2016**, 32 (24), 6074–6082.
37. Cevc, G.; Schätzleina, A.; Richardsen, H. Ultradeformable lipid vesicles can penetrate the skin and other semi-permeable barriers unfragmented. Evidence from double label CLSM experiments and direct size measurements. *Biochim. Biophys. Acta* **2002**, 1564 (1), 21–30.
38. Cevc, G.; Blume, G. Lipid vesicles penetrate into intact skin owing to the transdermal osmotic gradients and hydration force. *Biochim. Biophys. Acta* **1992**, 1104, 226-232.
39. Subongkot, T.; Pamornpathomkul, B.; Rojanarata, T.; Opanasopit, P.; Ngawhirunpat, T. Investigation of the mechanism of enhanced skin penetration by ultradeformable liposomes. *Int J Nanomedicine* **2014**, 25 (9), 3539-3550.
40. Loan Honeywell-Nguyen, P.; de Graaff, A.M.; Wouter Groenink, H.W.; Bouwstra, J.A. The in vivo and in vitro interactions of elastic and rigid vesicles with human skin. *Biochim. Biophys. Acta* **2002**, 1573, 130– 140.